CONF-9609111--1

UCRL-JC-123457
PREPRINT

IMPLICATIONS OF A "CROSS-ROLLED" YIELD SURFACE APPROXIMATION ON DEEP DRAWING

Roger W. Logan
University of California
Lawrence Livermore National Laboratory
Livermore, CA

NUMISHEET 96
Dearborn, MI
September 29 - October 3, 1996

March 1996

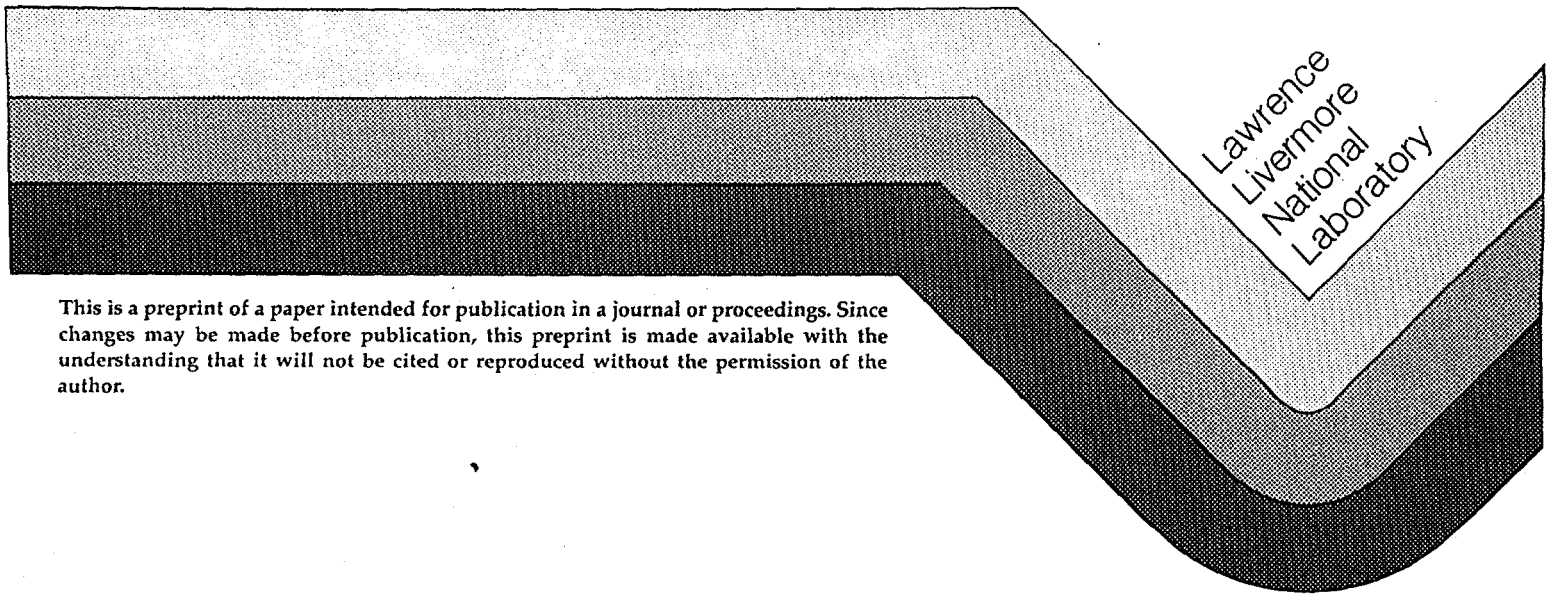

IMPLICATIONS OF A "CROSS-ROLLED" YIELD SURFACE APPROXIMATION ON DEEP DRAWING

Roger W. Logan
University of California
Lawrence Livermore National Laboratory
L-125 P.O. Box 808
Livermore, CA 94551

ABSTRACT

During deep-drawing, two issues manifest themselves that are due to normal and planar anisotropy in the sheet. These are a dependence of the Limiting Draw Ratio (LDR) on the average thinning ratio (R-value), and a dependence of ear formation and thinning around the circumference on the variation of R-value in the plane of the sheet. The quadratic (1948 Hill) yield surface has been applied to these issues and it has been demonstrated that there are numerous higher exponent yield criteria that may more closely duplicate experimental trends. These predict varying degrees of R-value dependencies of uniaxial yields and strength ratios in multiaxial loading paths. The result of this is that there are sometimes subtle and sometimes substantial differences in the predictions of the various yield surfaces on deep drawing regarding LDR and earing. Additional differences arise due to the way the shear term (45-degree yield) and the 0-degree vs. 90-degree strengths are treated in each criterion. These dependencies (in-plane strengths generated by the yield surfaces) are shown to affect the results of both LDR and earing during cupping. In particular, the 1979 Hosford and 1989 Barlat (Tricomponent) criteria, although identical for the normal anisotropy (planar isotropy) case, are strikingly different for cases where there are differences at 45 degrees and 90 degrees from the rolling direction.

INTRODUCTION AND YIELD SURFACES

In recent previous works (Logan, 1995 and 1996) we have outlined the implementation and use of various anisotropic yield criteria in explicit dynamics finite-element codes such as DYNA3D (Whirley, 1991) or ALE3D (Couch, 1995). Those yield criteria have included quadratic (Hill, 1948), higher-exponent (Hosford, 1979), and TriComponent (Barlat, 1989). All three of these yield criteria can be expressed in terms of a uniaxial flow stress X together with strain ratios from uniaxial tension or compression tests in various directions. We postulate the material coordinate system where a=rolling direction, b=transverse direction, and c=normal direction to the sheet, with strain ratios:

$$\begin{aligned} R &= R_0 = \varepsilon_b/\varepsilon_c \\ Q_{ab} &= R_{45} = \varepsilon_{b'}/\varepsilon_c \\ P &= R_{90} = \varepsilon_a/\varepsilon_c \\ Q_{bc} &= \varepsilon_{c''}/\varepsilon_a \\ Q_{ca} &= \varepsilon_{c'''}/\varepsilon_b \end{aligned} \qquad ...(1)$$

Here, the a'-b' coordinate system is obtained by rotating the a-b system 45° counterclockwise, the b''-c'' system by rotating the b-c system 45° counterclockwise, and the a'''-c''' system by rotating the a-c system 45° counterclockwise. R is measured in an a-direction uniaxial test, Q_{ab} in an a'-direction test, P in a b-direction test, Q_{bc} in a (hypothetical) b''-direction test, and Q_{ca} in a (hypothetical) a'''-direction test. In reality, Q_{bc} and Q_{ca} are not overly critical to sheet forming except with very tight bending radii, and a von Mises approximation is often used as it is here. Having measured or approximated the above strain ratios, we have all the needed constants for the quadratic 1948 Hill (H48) yield criterion:

$$\overline{\sigma}^2 = \frac{F(\sigma_b-\sigma_c)^2 + G(\sigma_c-\sigma_a)^2 + H(\sigma_a-\sigma_b)^2 + D}{R+1} \qquad ...(2)$$

Eqn. (2) relates the effective stress to the three normal components of Cauchy stress, with the term D containing the shear stress terms:

$$D = 2L\sigma_{bc}^2 + 2M\sigma_{ca}^2 + 2N\sigma_{ab}^2 \qquad ...(3)$$

The values for the constants in Eqns. (2) and (3) can be expressed in terms of above in-plane strain ratios for sheet forming, with the following additional relations needed:

$$\begin{aligned} F{=}S &= R/P \\ G &= 1 \\ H &= R \end{aligned} \qquad ...(4)$$

$$L = (Q_{bc} + \tfrac{1}{2})(R+1)$$
$$M = (Q_{ca} + \tfrac{1}{2})(R+S)$$
$$N = (Q_{ab} + \tfrac{1}{2})(1+S) \qquad \ldots(5)$$

The quadratic 1948 Hill criterion permits the relatively simple calculation of the ratio, $X(\theta)/X$, of the yield stress in a direction at an angle in the plane of the sheet to the rolling direction, as well as the calculated R-value in that direction:

$$\frac{X(\theta)}{X} = \left[\frac{R+1}{2Ns^2c^2 + R(c^2-s^2)^2 + c^4 + Ss^4}\right]^{1/2} \qquad (6)$$

$$R(\theta) = \frac{R + \{(2Q_{ab}+1)(1+S) - S - 1 - 4R\}s^2c^2}{Ss^2 + c^2} \qquad (7)$$

$$c = \cos(\theta)$$
$$s = \sin(\theta)$$

The R-value relation giving $R(\theta)$ is used in the implementation of the 1979 Hosford equation, extending 1948 Hill to a non-quadratic form with values of the exponent a in the range of a=8 for fcc (Hosford, 1979), and a =6 for bcc (Logan, 1980) metals:

$$\bar{\sigma}^a = \frac{F(\sigma_2-\sigma_3)^a + G(\sigma_3-\sigma_1)^a + H(\sigma_1-\sigma_2)^a}{R+1} \qquad (8)$$

Eqn. (8) is the second yield surface to be used in this study, with its implementation in DYNA3D discussed earlier (Logan, 1995). The advantages of the higher exponent in eqn. (8) have been discussed at length, and some of them are reviewed below; the higher exponent in itself allows an adequate fit to many (though not all) measured yield surfaces. However, difficulties arise in the implementation of the 1979 Hosford criterion for cases in other than principal stress/strain space. This stems from the lack of shear terms in the criterion. Eqn. (8) must remain in principal stress space to be used without spurious results and non-convexity problems. To do so, we must make a key approximation in updating the Cauchy stress tensor when using eqn. (8). The key necessity is a rotation to the principal stress coordinate space. It is straightforward to find and rotate the stress tensor to principal stress space, but to express eqn. (8) in that space we need to rotate the constants F, G, and H as well. To do so, we assume the dependence $R(\theta)$ as given for 1948 Hill by eqn. (7). The principal stress direction does not normally coincide with either the material (rolling and transverse direction) coordinate system, nor with the axes of principal strain. We assume that the axes of principal stress and strain approximately coincide, although for planar isotropy we know that they normally will not. However, this assumption, which leads us to ignore cross-terms in the constitutive matrix, is believed to lead only to small errors for the degree of anisotropy observed in most sheet metals. This is the assumption we use to update the stresses for the 1979 Hosford criterion.

In order to circumvent the stress space limitation of the 1979 Hosford criterion, Barlat and Lian (Barlat, 1989) introduced a criterion which offers all the advantages of the 1979 Hosford for the case of normal anisotropy (ΔR=0) but permits the introduction of a coupled shear term while retaining convexity of the yield surface and coordinate system invariance. This criterion is expressed below as in (Barlat, 1989), except that we retain the use of 'a' as the yield criteria exponent since many of our implementations refer to 'm' as a strain-rate exponent. Note also that to avoid confusion we have expressed the coefficient (2-c) explicitly:

$$\bar{\sigma}^a = \frac{(2-c)\left\{|K_1+K_2|^a + |K_1-K_2|^a\right\} + c|2K_2|^a}{2}$$

$$K_1 = \frac{\dot{\sigma_a} + h\dot{\sigma_b}}{2}$$
$$K_2 = \sqrt{\left(\frac{\dot{\sigma_a} - h\dot{\sigma_b}}{2}\right)^2 + p^2\sigma_{ab}^2} \qquad (9)$$

$$\dot{\sigma_a} = \sigma_a - \sigma_c$$
$$\dot{\sigma_b} = \sigma_b - \sigma_c$$

The Cauchy stresses must be defined to allow for a third (normal) stress, even though the implementation here is for the plane-stress shell element. This is because the plane-stress material routine is iterative so that even though the normal stress vanishes at convergence, we must recognize its presence during the iterations. Parameters c, h, and p^* may be defined in the current notation as follows:

$$c = 2\sqrt{\left(\frac{R}{1+R}\right)\left(\frac{P}{1+P}\right)}$$
$$h = \sqrt{\frac{R(1+P)}{P(1+R)}} \qquad \ldots(10)$$
$$p^* = \sqrt{\frac{(2Q_{ab}+1)(1+S)}{(1+R)(2+c)}}$$

The value of p is needed for the shear term in eqn (10). In the case of a=2, we have p=p*. However, this is also the case where the criterion reduces identically to 1948 Hill and is thus of interest only for verification. In general, the value of p* must be found iteratively as described in (Barlat, 1989). However, this has not been found to be a drawback for the case considered thus far where these coefficients are constant.

Given either of the choices of yield surface, the next step in implementation involves the stress update. For the isotropic case, this is conveniently done using the radial return method as discussed by Krieg and Key (Krieg, 1976). However, this method cannot be used directly for anisotropic plasticity. Thus, the incremental method described in (Bathe, 1982) and others is used in the DYNA3D and ALE3D implementations. Due to the small strain increments typical in an explicit dynamics code, this again is not a major drawback in computation speed.

If we consider the three yield criteria described above, that is the Hill 1948 (H48), Hosford 1979 (H79), and Barlat/Lian 1989 (B89), we can gain a quick insight into the tendencies of each by examining some of the simpler yet important stress ratios calculated by each. For example, at 45 degrees to the rolling direction, H48 predicts:

$$\frac{W}{X} = \frac{X(45^\circ)}{X} = \left[\frac{2(R+1)}{(S+1)(Q_{ab}+1)}\right]^{1/2}$$
$$\frac{W}{X} = \frac{X(45^\circ)}{X} = \left[\frac{R+1}{Q_{ab}+1}\right]^{1/2} (\forall R \equiv P) \qquad \ldots(11)$$

Similarly, H79 predicts a similar and simple relation at 45 degrees to the rolling direction :

$$\frac{W}{X}=\frac{X(45^\circ)}{X}=\left[\frac{R+1}{Q_{ab}+1}\right]^{1/a} \quad (\forall R \equiv P) \qquad ...(12a)$$

For the B89 criterion, there is no explicit formula for the ratio (*W/X*) ; its value tends to be intermediate between that predicted by H48 and H79. The value may be approximated by:

$$\frac{W}{X}=\frac{X(45^\circ)}{X}=\left[\frac{R+1}{Q_{ab}+1}\right]^{1/\sqrt{2a}} \quad (\forall R \equiv P) \qquad ...(12b)$$

We will see the manifestation of these trends below in the earing results. Since the exponent '*a*' is still *a*=2, Eqn. (11) shows a high dependence of yield stress on orientation in the plane of the sheet. This dependence is a likely factor in overprediction of earing as in (Logan, 1995), as the strong material in the 45 degree direction tends to pull in to form the wall of the punch (forming a deep trough), while compressing the 0 degree and 90 degree walls (forming high ears). The H79 equation (12) predicts much milder dependencies of strength ratios in stress states and directions other than tension in the rolling direction. At 90 degrees to the rolling direction, a similar situation exists for general values of unequal *R* and *P*:

$$\frac{Y}{X}=\frac{X(90^\circ)}{X}=\left[\frac{P(R+1)}{R(P+1)}\right]^{1/a} \qquad ...(13)$$

Eqn. (13) interestingly applies to all three criterion, but with a subtle twist. It predicts the value of (*Y/X*) for H48 with *a*=2, with a fairly strong dependence. The value of (*Y/X*) is also predicted for the H79 criterion with *a*>2 (typically *a*=6 or *a*=8), giving a mild dependence of (*Y/X*) on (*R/P*). For the B89 criterion, we can still use eqn. (13), but we must use it with *a*=2 regardless of the exponent chosen for the yield criterion itself. In other words, B89 gives the same strong (*Y/X*) variation as H48. This leads to subtle differences in values of Limiting Draw Ratio (LDR) and Goss-texture (Malin, 1993) earing magnitudes (ears at 0 degrees relative to ears at 90 degrees).

In biaxial tension, where $\sigma_a = \sigma_b = B$, both 1948 Hill and 1979 Hosford predict the relatively simple value:

$$\frac{B}{X}=\left(\frac{R+1}{S+1}\right)^{1/a} \qquad ...(14)$$

Clearly, values of $a > 2$ will give a much milder dependence often observed experimentally and thus should provide better correlation with LDR as shown in previous works. The value of (*B/X*) for the B89 criterion has a more complex form:

$$\frac{B}{X}=\left(\frac{2}{(2-c)(1+h^a)+c(1-h)^a}\right)^{1/a} \qquad ...(15)$$

Eqn. (15) simplifies exactly to eqn. (14) for the case of *R*=*P*, thus providing B89 with the same mild dependence of (*B/X*) on *R* as shown by H79. Graphical examples of these trends in stress ratio are shown in Fig. 1 for two materials with hypothetical sets of *R*-values taken from Table 1 below. The experimental data sets in Table 1 are taken from Wilson and Butler (Wilson, 1962); the contrived data sets have been adjusted to show particular numerical points. The numbers chosen are representative of available sheet materials but adjusted to provide exactly *R*=*P* in one case (material Sb), and exactly ΔR=0 in another case (material Nm). This allows us to clearly separate the subtleties of the different yield criteria.

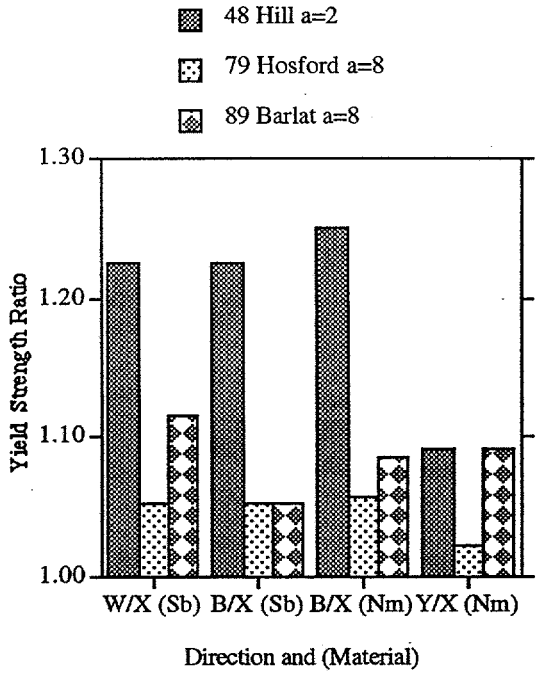

FIG. 1. COMPARISON OF STRENGTH RATIOS PREDICTED USING PLANE STRESS YIELD CRITERIA (H48, H79, B89) FOR MATERIALS WHERE *R*=*P* (SB), AND WHERE *R*<*P* WITH ΔR=0 (NM).

Note that in Fig. 1, the H48 criterion predicts strong strength ratio dependencies in all cases, and the H79 criterion predicts very mild dependencies. In general, the B89 criterion agrees with H79 for the *B/X* ratio, with H48 for the *Y/X* ratio, and is intermediate for the *W/X* ratio. Note that for the "Nm" material, B89 is again somewhat intermediate between H48 and H79 since *R*<<*P* for this case ; note again the values of *R* for the two contrived materials in Fig. 1, the "Sb" and "Nm" sets.

In the following sections we will demonstrate the effect of the chosen yield surface (H48, H79, or B89) on the extent of earing in cupping with a "cross-rolled" texture, the nature of the LDR dependence for that case and cases where $R \neq P$, and on the earing trends that might be observed for materials fitted to these yield surfaces in cases where $R \neq P$.

TABLE 1. PLASTIC ANISOTROPY FOR CONTRIVED AND REAL MATERIAL DATA SETS USED IN THIS WORK.

Matl	R	Q_{ab}	P	$\bar{R}$	$\frac{\Delta R}{R}$	$\frac{\Delta P}{R}$	$\frac{\Delta P}{P}$	$\frac{R}{P}$
Materials Used in Fig. 1 - Contrived								
Sa	4.00	1.00	4.00	2.50	1.20	0.00	0.00	1.00
Sb	2.00	1.00	2.00	1.50	0.67	0.00	0.00	1.00
Sc	1.50	1.00	1.50	1.25	0.40	0.00	0.00	1.00
Sd	0.50	1.00	0.50	0.75	-0.67	0.00	0.00	1.00
Se	1.00	2.00	1.00	1.50	-0.67	0.00	0.00	1.00
Sf	0.50	2.00	0.50	1.25	-1.20	0.00	0.00	1.00
Materials Used in Fig. 4-7 - Contrived								
Nf	4.00	1.00	4.00	2.50	1.20	0.00	0.00	1.00
Nj	1.00	2.00	3.00	2.00	0.00	-1.00	-1.00	0.33
Nk	0.50	2.00	1.50	1.50	-0.67	-0.67	-1.00	0.33
Nt	1.00	1.00	2.00	1.25	0.40	-0.80	-0.67	0.50
Nm	1.50	2.00	2.50	2.00	0.00	-0.50	-0.50	0.60
Nn	1.00	4.00	1.00	2.50	-1.20	0.00	0.00	1.00
Nu	0.68	1.31	0.68	0.99	-0.64	0.00	0.00	1.00
Materials Used in Fig. 4-7 - W&B Experiments								
Wp	0.77	1.31	0.58	0.99	-0.64	0.19	0.28	1.33
Wb	0.82	0.86	0.89	0.86	-0.01	-0.08	-0.08	0.92
Ws	1.49	1.18	1.92	1.44	0.36	-0.30	-0.25	0.78
Wc	0.86	0.33	1.02	0.64	0.96	-0.25	-0.17	0.84

EARING: CROSS-ROLLED ASSUMPTION

To compare the different yield criteria in DYNA3D and ALE3D with earing observed experimentally, we compare the data obtained by Wilson and Butler (Wilson, 1962) with that obtained using simulations with either a =2 in eqn. (2) (H48), a =8 in eqn. (8) (1979 Hosford), or a =8 in eqn. (9) (1989 Barlat). Numerous runs with $R = P$ were made as outlined in detail previously (Logan, 1996) for the three criteria outlined here, using a 100mm punch and 200mm diameter blank, and the R-values as stated in Table 1 under data for Fig. 2. In all cases, a rolling-direction yield of 200MPa, tangent modulus of 250MPa, sheet thickness of t=0.80mm, and friction coefficient of 0.100 was used with punch nose and die lip radii of r=6.35mm, providing an (r/t)=8 in order to minimize the complicating effect of bending.

The stress ratio dependencies illustrated in Fig. 1 can help to intuitively explain the correlation of the various yield surfaces with experimental (W&B) earing results shown in Fig. 2. As explained above in reference to eqns. (11-12), the high (relative to most experimental observations) strength ratios predicted by H48 lead to an overprediction of earing on planar anisotropy. In this context, we quantify the 4-fold earing with ears at 0 and 90 degrees and troughs at 45 degrees as:

$$E45 = \Delta h / h$$
$$\Delta h / h = \frac{2*(h00 - 2*h45 + h90)}{(h00 + 2*h45 + h90)} \qquad \ldots(16)$$
$$\Delta R = (R - 2*Q_{ab} + P)/2$$
$$\bar{R} = (R + 2*Q_{ab} + P)/4$$

The quantities $E45$ and $\Delta R / \bar{R}$ are then correlated to produce the earing trend lines shown in Fig. 2. As expected from its intermediate stress ratio behavior, the earing trend line for B89 is intermediate between H48 and H79, the latter of which correlates best to the experimental data.

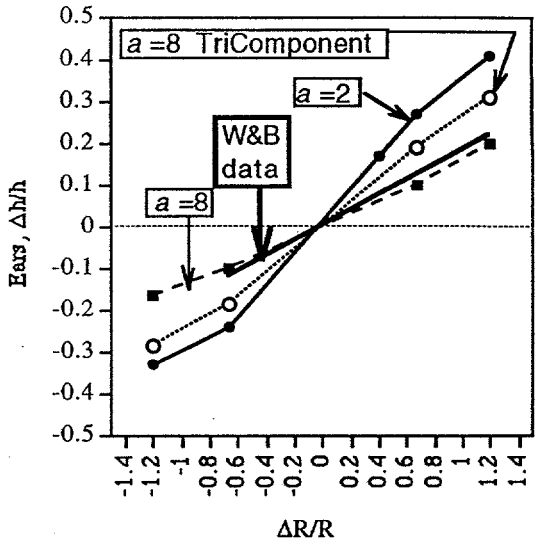

FIG. 2. PLOT OF EARING (ΔH/H VS. ΔR/R) INCLUDING WILSON AND BUTLER DATA COMPARED TO ALE3D AND DYNA3D RESULTS WITH A =2 (48 HILL), A =8 (79 HOSFORD) AND A =8 (89 BARLAT).

(PLANAR) ANISOTROPY AND THE LDR

Another strong effect of anisotropy in deep drawing occurs with the observed dependence of the Limiting Draw Ratio (LDR) on the R-value(s) of the sheet. The LDR is defined as the ratio of maximum (limiting) blank diameter to punch diameter in cylindrical cupping. This dependence was shown with experimental data and axisymmetric finite-element calculations in previous work (Logan, 1987). In Fig. 3, the experimental data in (Logan, 1987) is reproduced, along with calculations performed with DYNA3D using the H48, H79, and B89 criteria. For this case, with $R = Q_{ab} = P = \bar{R}$ set intentionally, the H79 and B89 should in fact give identical results. In fact, there is a slight difference between the two which we attribute to perhaps the numerical rounding associated with the coincident principal stress and principal strain assumption. Nonetheless, both show a much milder dependence than H48. Although these trends are essentially the same as those shown in (Logan, 1987), the three-dimensional implementation now allows us to examine the LDR in a deeper way. The experiments performed by Meuleman and reported in (Logan, 1987) were divided into three categories, depending on the magnitude of the quantity $\Delta R/\bar{R}$, as shown in Fig. 3. Somewhat surprisingly, there is no discernible affect of $\Delta R/\bar{R}$ on the LDR as viewed in Fig. 3. To see if the numerical simulations and chosen yield criteria concur, we repeated the LDR simulations and plotted data points at $\bar{R} = 0.5, \bar{R} = 2.0$ as above with an imposed value of $\Delta R/\bar{R} = 0.4$ to explore the affect of planar anisotropy as predicted by each yield surface. The H48 criterion shows a significant increase in LDR with $\Delta R/\bar{R} = 0.4$, in contrast to the experimental data and perhaps our intuition as well. The H79 criterion shows only a very slight increase in LDR, while B89 actually shows a slight decrease. The divergence of H79 and B89 as $\Delta R/\bar{R}$ is increased is not surprising due to their different nature as explained in eqns. (12-13) above. What is perhaps most

striking is the minimal affect of $\Delta R/\overline{R}$ on the LDR in general, as observed both experimentally and by the two high-exponent yield criteria. We must bear in mind that nonzero $\Delta R/\overline{R}$ will inevitably lead to ears and troughs thus lowering the trimmed cup height as explored in (Logan, 1996).

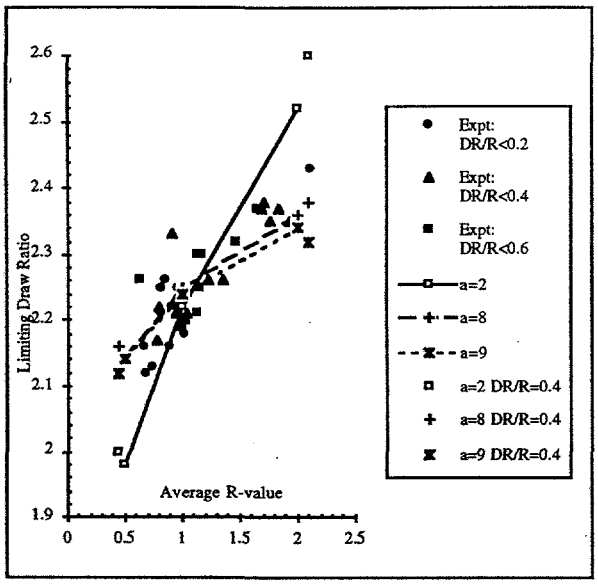

FIG. 3. EFFECT OF $\overline{R}$ AND $\Delta R/\overline{R}$ ON THE LDR AS SHOWN EXPERIMENTALLY AND BY THE THREE YIELD CRITERIA (H48 LABELED A=2, H79 LABELED A=8, AND B89 LABELED A=9; EXPONENT IS STILL A=8).

EARING: EFFECT OF UNEQUAL R AND P

Although the numerical trend lines of earing (E45 in eqn. 16) shown in Fig. 2 were obtained with R=P, this is rarely exactly the case. In order to explore the effect of unequal R and P, some of the actual values reported in (Wilson, 1962) along with some contrived cases with R<P were run with DYNA3D, and the results plotted in Fig. 4a-b. With the simulation results connected point-by-point in Fig. 4a, we see that although the value of $\Delta P = R - P$ can locally affect the value of $\Delta h/h$ (E45), overall the regression lines shown in Fig. 4b agree with the observations of Fig. 2 where R=P. In the cases of unequal R and P, we now have another type of earing as well, that in its extreme will lead to Goss-texture behavior with ears at 0 and 180 degrees and troughs at 90 and 270 degrees (Malin, 1993). This earing may be quantified by:

$$E90 = \Delta h(0-90)/h$$

$$\Delta h(0-90)/h = \frac{4(h00-h90)}{(h00+2*h45+h90)} \qquad ...(17)$$

$$\Delta P = R - P$$

$$\overline{P} = (R+P)/2$$

In Fig. 5a-b, we attempt to correlate E90 with the quantity $\Delta P/\overline{R}$. Two things are readily evident. First, the correlation in general (as noted by the regression values of r^2) are not very good. Second, the highest dependence is shown by B89, rather than the usual winner, H48, in such dependencies. Overall H79 shows the least dependence of E90 on $\Delta P/\overline{R}$; this at first seems intuitively satisfying, but a simple "flange in compression" earing analysis will show the opposite trend, as discussed below. In Fig. 6a-b, we correlate E90 instead with the quantity $\Delta P/\overline{P}$ as defined by eqn. (17) above. There is in general still considerable scatter, although even the point-to-point plot in Fig. 6a looks smooth for H79. The regression lines in Fig. 6b show the same qualitative results as in Fig. 5b, with the r^2 coefficients much improved for B89 and H79. Alternately, we can correlate E90 with the ratio R/P as shown in Fig. 7a-b. Again, the point-to-point plot in Fig. 7a is smooth only for the H79 case, and the regression fits are quite good for both B89 and H79. The trend of strength of dependencies, B89 strongest and H79 weakest, remains as it did in Fig. 6.

DISCUSSION OF CALCULATED E90 TRENDS

Intuitively, we might at first be satisfied with the mild dependence shown by H79 in Figs. 4-7, and surprised by the strong dependence of E90 on $\Delta P/\overline{P}$ etc. shown by B89. Unfortunately, more experimental data is desperately needed in this area and will be a topic of future work. Meanwhile, in an attempt to numerically resolve these observations, we consider here a very simple earing analysis. We will choose two of the contrived materials (Nf and Nj) from Table 1, and examine the DYNA3D predictions of E45 and E90 in Table 2:

TABLE 2. TRENDS IN E45 AND E90 EARS PREDICTED BY DYNA3D.

Matl.	R	Q_{ab}	P	Earing	H48	H79	B89
Nf	4	1	4	E45=	.396	.259	.300
Nj	1	2	3	E45=	-.110	-.060	-.070
Nj	1	2	3	E90=	.091	.046	.128

Material Nf, with $\Delta R/\overline{R} = 1.20$, shows the expected trend of E45 shown in Fig. 2. That is, H48 shows the most E45, B89 slightly less, and H79 least of all and closest to the experimental trend. The E90 earing is null in each case since R=P exactly. The trends for material Nj are particularly interesting, and are plotted graphically in Fig. 8 with the value $\Delta P/\overline{P} = 1.0$ for the Nj material; the material Nm shows the same trend with its $\Delta P/\overline{P} = 0.5$ although to a lesser extent than for material Nj. These materials have $\Delta R/\overline{R} = 0.00$, but they do exhibit some degree of 4-fold E45 earing, with ears at about 45 degrees and "troughs" at 0 and 90 degrees, although in most cases for Nm and Nj, the height at 0 degrees is nearly as high as the height at 45 degrees. Nevertheless, when defined as in eqn. (16), E45 again follows the familiar trend of H48 highest, with B89 intermediate and H79 the smallest magnitude.

Since R<<P for material Nj, we can examine the trends of E90 with the various yield criteria as shown above in Figs. 4-7. For both materials Nm and Nj, the same trends in E90 predictions of the three yield criteria are observed; these trends continue in the other materials where $R \neq P$ as well. The tendency is that H48 shows an E90>0, nearly proportional to $\Delta P/\overline{P}$. The B89 criterion shows an even greater E90, instead of the reduction vs. H48 observed in predicting E45. The H79 criterion shows much less E90 than either. From our experience with the trend of these three yield criteria in predicting E45, B89 would seem to be the outlier if the same ordering (H48 most earing, H79 least) held true for E90. Our intuition for E45 was based simply on the predicted value of W/X for each yield criterion. However, for E90, the situation is complicated since $Y \neq X$. Thus, our intuition must now encompass the strength ratios in Table 3 for material Nj.

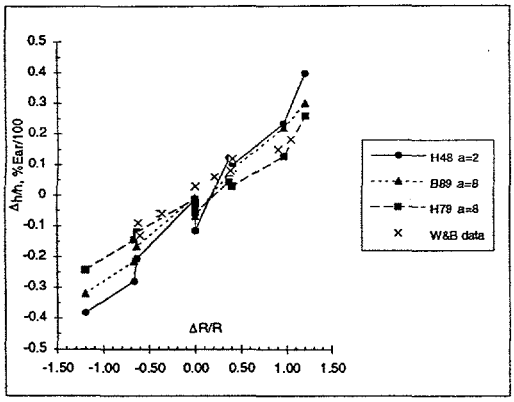

FIG. 4A) E45 CORRELATION, RAW DATA SETS.

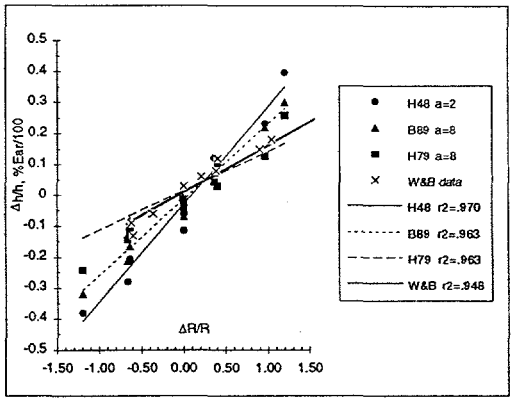

FIG. 4B) E45 CORRELATION, REGRESSION FITS.

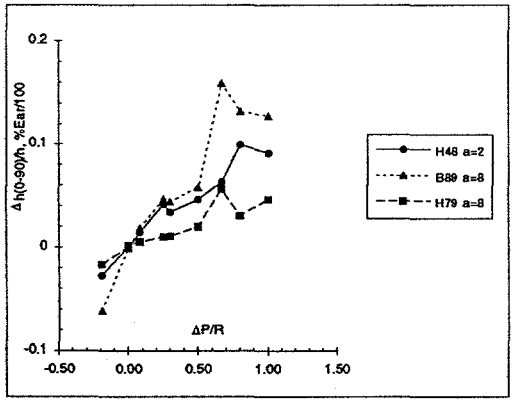

FIG. 5A) E90 CORRELATION, RAW DATA SETS.

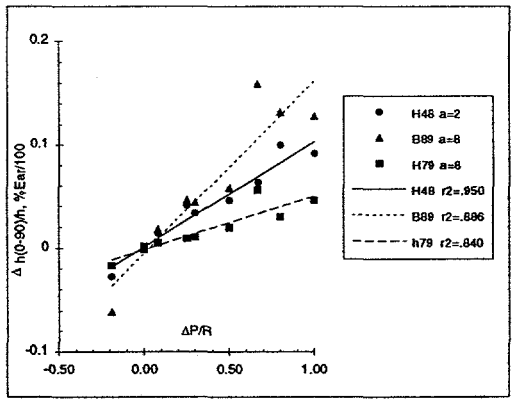

FIG. 5B) E90 CORRELATION, REGRESSION FITS.

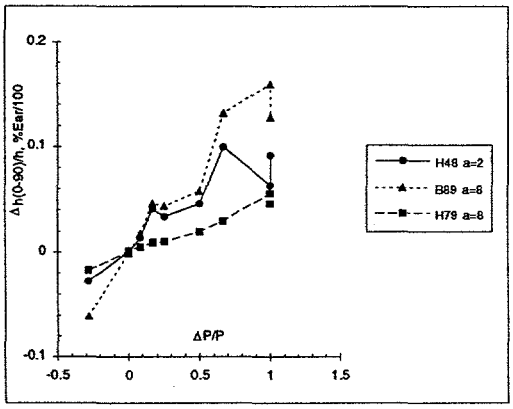

FIG. 6A) E90 CORRELATION, RAW DATA SETS.

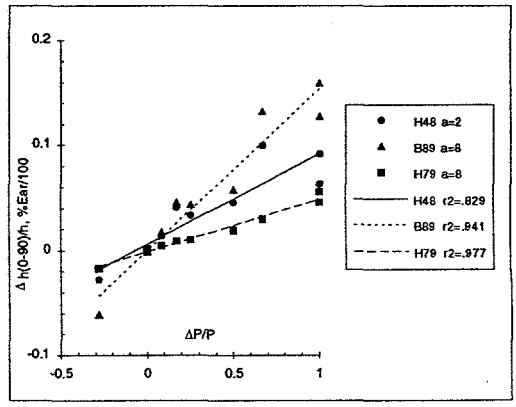

FIG. 6B) E90 CORRELATION, REGRESSION FITS.

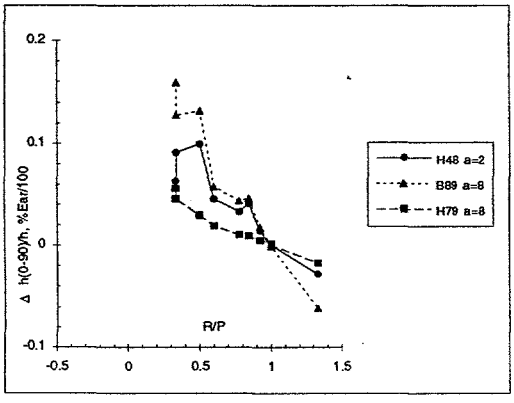

FIG. 7A) E90 CORRELATION, RAW DATA SETS.

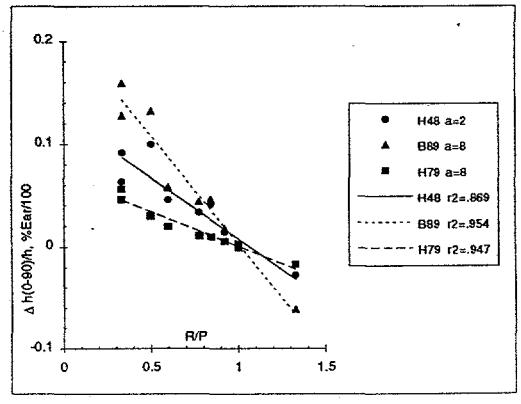

FIG. 7B) E90 CORRELATION, REGRESSION FITS.

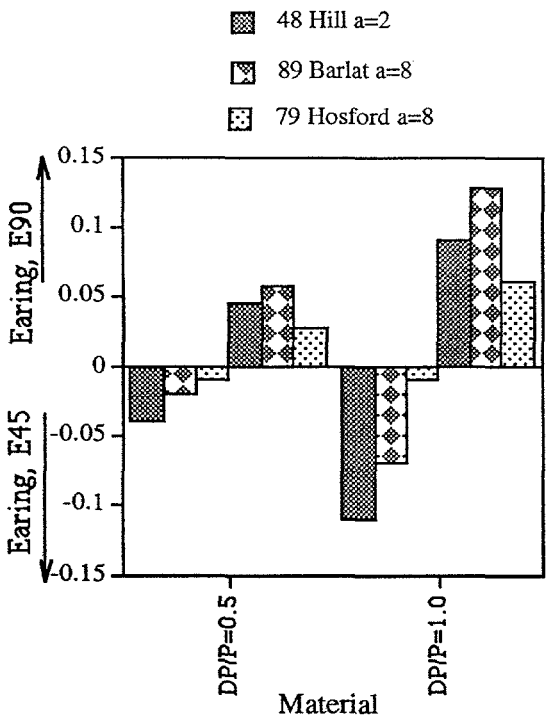

FIG. 8. PREDICTED DEPENDENCE OF EARING (E45 AND E90) ON THE CHOSEN YIELD CRITERIA FOR DIFFERENT $\Delta P / \bar{P}$.

TABLE 3. CALCULATED STRENGTH RATIOS FOR MATERIAL NJ: R=1, Q_{AB}=2, P=3.

Ratio:	H48	H79	B89
X/X	1.000	1.000	1.000
W/X	1.000	1.000	1.049
Y/X	1.225	1.052	1.225

Using the same "flange in uniaxial compression" intuition that works qualitatively for E45, we can understand or at least explain why E90>0 for all three criteria; even though *Y/X*>1 giving less hoop compressive strain in the 0 degree ear, *P*=3 so there is much more lateral expansion, in the radial or ear direction for the 0 degree ear, as compared with the 90 degree ear where we have an *R*=1 compression test. Further, we can see why B89 would show more E90, since it predicts a stronger 45 degree hoop strength *W/X*. Less hoop compression at 45 degrees means more at 0 and 90 degrees and an exaggerated E90 compared with H48. This logic cannot explain the much-reduced E90 predicted by H79 with DYNA3D. In fact, since H79 predicts a lower *Y/X*=1.052, we would expect more hoop compression at 0 degrees and thus a higher value of E90 and perhaps even B89. A simple earing program was written to show this, and the results are shown in Table 4:

TABLE 4. TRENDS IN E45 AND E90 EARS PREDICTED BY UNIAXIAL COMPRESSION EAR ANALYSIS.

Matl.	R	Q_{ab}	P	Earing	H48	H79	B89
Nf	4	1	4	E45=	.414	.238	.295
Nj	1	2	3	E45=	-.080	-.034	-.057
Nj	1	2	3	E90=	.040	.117	.045

In essence, this simple earing program envisions the 0, 45, and 90 degree directions in a cup undergoing a uniaxial compression test. The 45 degree direction is weighted twice, and we then demand a hoop force balance as the rim of the blank as a whole must see a hoop strain of $\varepsilon_H = \ln(d_p / d_b)$, where d_p=punch diameter, and db=blank diameter. The individual hoop strains ε_H^{00}, ε_H^{45}, and ε_H^{90} are adjusted to achieve a force balance in the hoop direction; as the magnitude of each of the compressive ε_H^{θ} increases, strain hardening increases the respective σ_H^{θ}. Further, thickening (depending on the local $R(\theta+90)$ value, as $1/(R(\theta+90)+1)$), and widening (as $R(\theta+90)/(R(\theta+90)+1)$) increases the hoop force F_H^{θ}. The width and thickening effects can be modulated by adjustables α_w and α_t, where $0 \le \alpha_i \le 1$. As shown in Table 4, with $\alpha_w = 0.5$ and $\alpha_t = 1.0$ as a best fit, this very simple ear analysis is able to reproduce, with fair quantitative agreement, the trends in E45 as shown by DYNA3D. The simple analysis also predicts that B89 should indeed have higher E90 than H48. The "higher" B89 dependence now seems to make sense. However, regardless of the values of α_w and α_t chosen, the simple ear analysis says that H79 should show the highest E90 of all; this is the opposite of the finite element predictions. And yet, examining the strength ratios in Table 3, it does seem that E90 could be greater for H79, since the weak ear at 0 degrees will be squeezed out taller for H79 versus H48 or perhaps even B89. Either DYNA3D is leading us astray or a more complex ear analysis is required to capture the E90 trends. Such an analysis has been presented in (Van Houtte, 1993); a simplified extension of the above is added here in that spirit. In simple terms, we assume that although part of the deforming cup is in uniaxial compression, much of it has at least some component of uniaxial tension in the radial direction. In fact, there is some component, picked by another adjustable α_R in this analysis, of uniaxial tension all the way out to the flange. Assuming that material is flowing in the respective 0, 45, and 90 degree directions, we can find the uniaxial tension flow stress in the radial direction as a function of *W/X* or *Y/X* from eqns. (11-13); this is further modified by strain hardening due to plastic work assumed to occur in the hoop direction at these respective locations. (Naturally a coupled analysis would be more accurate, and perhaps require less adjustables, but separating the terms and effects does allow an increased intuitive feel). We can then back out a pseudo-radial strain ε_R^{θ} from this pseudo-radial stress σ_R^{θ}. The result of this, as shown in Table 5, is a strong effect on E45 and E90; the correction to E90 is such that for any value of adjustable α_R, ($\alpha_R = 0.25$ used in Table 5) the trends of E90 now agree with DYNA3D; that is, H79 shows the least E90 of all.

TABLE 5. TRENDS IN E45 AND E90 EARS PREDICTED BY UNIAXIAL COMPRESSION PLUS RADIAL TENSION EAR ANALYSIS.

Matl.	R	Q_{ab}	P	Earing	H48	H79	B89
Nf	4	1	4	E45=	.476	.159	.262
Nj	1	2	3	E45=	-.084	-.030	-.039
Nj	1	2	3	E90=	.105	.059	.114

Clearly, our simple intuition may fail us as the nature of earing and yield criteria become more complex. However, it seems worthwhile to find at least a qualitative simple solution

that allows our intuition to explain the finite-element or experimental trends.

CONCLUSIONS

Numerical simulations of the Limiting Draw Ratio and Earing phenomena during cupping have shown that many of the trends for fully "cross-rolled" materials, i.e. $R = P$, are intuitive, whereas the trends created when $R \neq P$ (more typical or real sheet materials) are often not intuitive. In general, the H79 criterion seems to correlate best with available earing data; B89 is also reasonable and has a relatively simpler implementation. Both of these criterion give good correlation with data on LDR dependence. More work is needed on experimental and numerical trends of earing when $R \neq P$ to see what is the best fit to trends of the data, in light of the complex earing interactions that occur in this circumstance.

ACKNOWLEDGMENTS

The author wishes to thank W.F. Hosford and D.D. Sam for helpful discussions regarding anisotropy. The efforts of G.J. Leake, L.D. McMichael, and R.G. Couch are noted in preparation of the ALE3D simulations. This work was performed under the auspices of the U.S. Department of Energy by the Lawrence Livermore National Laboratory under contract W-7405-Eng-48.

REFERENCES

Barlat, F. and Lian, J. (1989), "Plastic Behavior and Stretchability of Sheet Metals, Part I: A Yield Function for Orthotropic Sheets Under Plane Stress Conditions", *Int. J. Plasticity* 5, pp. 51-66.

Bathe, K.J. (1982), *Finite Element Procedures in Engineering Analysis*, Prentice-Hall, Englewood Cliffs, N.J.

Couch, R.G., McCallen, R.C., Otero, I.J., and Sharp, R.W. (1995), "3D Metal Forming Applications of ALE Techniques", in *NUMIFORM 95* Proceedings, June 18-21, Ithaca, NY, ed. S.F. Shen and P.R. Dawson, Balkema publishers, Rotterdam, p.401.

Hill, R. (1948), *The Mathematical Theory of Plasticity*, Clarendon Press, Oxford.

Hosford, W.F. (1979), "On Yield Loci of Anisotropic Cubic Metals", Proc. 7th N. Amer. Metal Working Research Conf., SME, Dearborn p. 191.

Krieg, R.D. and Key, S.W. (1976), "Implementation of a Time Dependent Plasticity Theory into Structural Computer Programs", Vol. 20 of *Constitutive Equations in Viscoplasticity: Computational and Engineering Aspects*, ASME, New York, NY, p.125.

Logan, R.W., and Hosford, W.F. (1980), "Upper-Bound Anisotropic Yield Locus Calculations Assuming [111] Pencil Glide", *Int. J. Mechanical Sci.* 22, p.419.

Logan, R.W., Meuleman, D.J., and Hosford, W.F. (1987), "The Effects of Anisotropy on the Limiting Drawing Ratio", in *Formability and Metallurgical Structure*, eds. A.K. Sachdev and J.D. Embury, TMS-AIME, p.159.

Logan, R.W. (1995), "Finite-Element Analysis of Earing Using Non-Quadratic Yield Surfaces", in *NUMIFORM 95* Proceedings, June 18-21, Ithaca, NY, ed. S.F. Shen and P.R. Dawson, Balkema publishers, Rotterdam, p.755.

Logan, R.W. (1996), "Use of Non-Quadratic Yield Surfaces in Design of Optimal Deep-Draw Blank Geometry", SAE paper 960597, in *Sheet Metal Stamping for Automotive Applications*, SP-1134, SAE, Warrendale, PA, p.61.

Malin, A.S. and Chen, B.K. (1993), "Six-Fold Symmetry in Deep Drawn Cups (AA3004)", in *Aluminum Alloys for Packaging*, ed. J.G. Morris, H.D. Merchant, E.J. Westerman, and P.L. Morris, TMS p.251.

Van Houtte, P., Clarke, P., and Saimoto, S. (1993), "A Quantitative Analysis of Earing During Deep Drawing", in *Aluminum Alloys for Packaging*, ed. J.G. Morris, H.D. Merchant, E.J. Westerman, and P.L. Morris, TMS p.261.

Whirley, R.G., and Hallquist, J.O. (1991), "DYNA3D: A Nonlinear, Explicit, Three-Dimensional Finite Element Code for Solid and Structural Mechanics- User Manual," University of California, Lawrence Livermore National Laboratory, Report UCRL-MA-107254.

Wilson, D.V. and Butler, R.D. (1962), "The Role of Cup-Drawing Tests in Measuring Drawability", *J. Inst. Metals* 90, p. 473.